

#### A-1.1.4 Development of Visible Spectrometer to Measure Nitrogen Oxides

**Contact Person** Yutaka Kondo  
Professor  
Solar Terrestrial Environment Laboratory, Nagoya University  
Honohara, Toyokawa, Aichi 442, Japan  
Phone +81-5338-6-3154, Fax +81-5338-6-0811  
E-mail

**Total Budget for FY1994 - FY1996** 37,628,000 Yen (FY1996; 12,804,000 Yen)

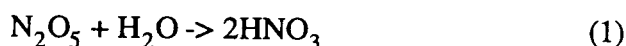
#### Abstract

The importance of the stratospheric nitrogen chemistry is recognized related to the heterogeneous reactions in both polar and mid-latitude regions. Daily measurements of slant column amounts of NO<sub>2</sub> and O<sub>3</sub> continues successfully at Kiso Observatory (36°N, 138°E) of the University of Tokyo from November 1992. Slant column amounts of NO<sub>2</sub> and O<sub>3</sub> measurements at Rikubetsu (43°N, 144°E) started April 1994. The data obtained at Rikubetsu and Moshiri Observatory (44°N, 142°E) show good agreement. A stellar occultation spectrometer has been developed and tested its performance using stars in Tokyo.

**Key Words** NO<sub>2</sub>, NO<sub>x</sub>, Visible Spectrometer, Pinatubo, Heterogeneous Reaction, A stellar occultation spectrometer

#### 1. Introduction

Recent laboratory studies have suggested that the heterogeneous reaction



on the surface of the sulfate aerosols can convert reactive nitrogen into HNO<sub>3</sub> efficiently. Since the reaction probability of reaction (1) is fairly insensitive to H<sub>2</sub>SO<sub>4</sub> fraction in an aerosol particle (H<sub>2</sub>SO<sub>4</sub>/H<sub>2</sub>O), it is also insensitive to temperature. Therefore, reaction (1) has the potential to greatly reduce reactive nitrogen globally, even under background aerosol conditions. The reduction of reactive nitrogen (NO<sub>x</sub>) leads to an increase in active chlorine (Cl<sub>x</sub>) through a reduction of the following reaction.



Similarly, the reduction of NO<sub>x</sub> also result in an increase of odd hydrogen (HO<sub>x</sub>). Consequently, the relative importance of Cl<sub>x</sub> and HO<sub>x</sub> catalyzed ozone destruction increases while that of NO<sub>x</sub> catalyzed destruction decreases. With this higher contribution of Cl<sub>x</sub> catalyzed ozone loss, the known growth in anthropogenic chlorine is considered to be a plausible explanation for the observed downward ozone trend, especially at mid-latitudes.

The eruption of Mount Pinatubo (15°N, 120°E) injected large amounts of SO<sub>2</sub> into the stratosphere in June 1991. Subsequently, H<sub>2</sub>SO<sub>4</sub> aerosols were formed from SO<sub>2</sub>, whose mass was observed to be 2 to 2.5 times larger than that of El Chichon. The increase in surface area of sulfate aerosols in the stratosphere due to the Pinatubo volcanic eruption provides an excellent opportunity to

test our understanding of these heterogeneous reactions and in turn, their role on background aerosols.

Simultaneous measurements of NO<sub>2</sub> and O<sub>3</sub> with a high accuracy and on a long time base are essential to study the effect from the heterogeneous reactions on the O<sub>3</sub> chemistry and trend. In this study, we have made a systematic assessment on the accuracy and precision of the NO<sub>2</sub> and O<sub>3</sub> measurements by the ground base visible spectrometers.

It is also important to carry out campaign style observations of those nighttime variation. It is because the nitrogen pentoxide (N<sub>2</sub>O<sub>5</sub>) which is one of key species in the heterogeneous reaction is produced in nighttime. Though it is difficult to measure N<sub>2</sub>O<sub>5</sub>, the production rate of N<sub>2</sub>O<sub>5</sub> can be evaluated from the time variation of NO<sub>2</sub> and NO<sub>3</sub>. In this study, we have been developing a remote sensing system to observe the nighttime variation of nitrogen oxides (NO<sub>2</sub>, NO<sub>3</sub>) and O<sub>3</sub>.

## 2. Long term measurements of NO<sub>2</sub> and NO<sub>3</sub> by visible spectrometer

NO<sub>2</sub> and O<sub>3</sub> have characteristic absorption features in the visible wavelength region. Stratospheric NO<sub>2</sub> and O<sub>3</sub> column amounts can be measured at sunrise and sunset by observing scattered sunlight in the visible region coming from the zenith sky.

Measurements of the stratospheric NO<sub>2</sub> and O<sub>3</sub> started at Moshiri Observatory (44.4°N, 142.3°E) in April 1991 and Rikubetsu Observatory (43.5°N, 143.8°E) in April 1994. These two observatories are located with a distance of about 150 km. However weather condition is not always the same; for example, there are many more clear days at Rikubetsu than at Moshiri during winter. A possible influence from the tropospheric pollution on the NO<sub>2</sub> measurement may differ between the two measurements. Because of the close locations of the two observatories with these somewhat different conditions of the measurements, these data sets give a good opportunity to evaluate the overall accuracy of the measurements. The O<sub>3</sub> data are also compared with the O<sub>3</sub> measurements made by a Dobson spectrometer at Sapporo (43.1°N, 141.3°E) by Japan Meteorological Agency.

### 2.1 NO<sub>2</sub> measurements

A correlation plot between the two NO<sub>2</sub> measurements made between April 1994 and March 1995 is shown for sunrise (AM) and sunset (PM) in Figures 1a and 1b, respectively. A good agreement with a square of a correlation coefficient ( $r^2$ ) of 0.94 and 0.92 is seen. When a linear relation without a constant term is fitted to the data by a least square calculation, the slope becomes  $0.999 \pm 0.004$  and  $1.012 \pm 0.004$  for AM and PM data, respectively, suggesting very small systematic differences between the two measurements.

A part of the random disagreement in the individual data may be due to a real difference in the stratospheric NO<sub>2</sub> values. Consequently, the difference found here can be considered as the upper limit of the precision of the measurements. The root mean square difference between the two measurements is  $0.36 \times 10^{16} \text{ cm}^{-2}$  for the AM data and  $0.54 \times 10^{16} \text{ cm}^{-2}$  for the PM data. Assuming that the difference results from the same amount of errors of the two measurements, the precision of the individual measurement becomes  $1/\sqrt{2}$  of the difference, *i.e.*,  $0.26$  and  $0.38 \times 10^{16} \text{ cm}^{-2}$ . These values correspond to 4 - 9 % of the slant column amounts for both the AM and PM NO<sub>2</sub> measurements. The percent error is larger in winter because of the smaller column amounts. The upper limit precision shown here are slightly larger than the precision of  $0.2 \times 10^{16} \text{ cm}^{-2}$  estimated from the spectrum fitting.

The apparent correlation in Figures 1a and 1b is because the range of the NO<sub>2</sub> seasonal variation is larger than the deviation of the data around the linear fit. To evaluate an agreement between the day to day variations within each month, a 31-day running mean value was removed from the original daily data and the residual variations were compared. The residual variations still agree with  $r^2$  value of 0.40 and 0.34 for AM and PM data, respectively. This means that the two measurements show a common day to day variation to some extent. Consequently, the precision of

the NO<sub>2</sub> measurement is considered to be good enough to detect the day to day variation of the stratospheric NO<sub>2</sub>.

## 2.2 O<sub>3</sub> measurements

The daily O<sub>3</sub> slant column amounts observed at Moshiri from April 1991 to March 1995 is shown in Figure 2. The seasonal maximum and minimum of O<sub>3</sub> column amount appear in March and September, respectively. In this figure the Dobson O<sub>3</sub> data at Sapporo are also shown. To match the Y-axis of these two data sets, an air mass factor of 17.5 is chosen. In general, shapes of both the seasonal variations agree well. Between the end of 1991 and middle of 1992, the O<sub>3</sub> values obtained by the visible spectrometer were systematically lower than the Dobson values when the air mass factor of 17.5 is used. This is probably due to the radiative effect of Pinatubo volcanic aerosols.

Correlation plot between the O<sub>3</sub> values obtained at Moshiri and Rikubetsu is shown in Figure 3. Daily values obtained between April 1994 and March 1995 are used for this figure. In this figure a good agreement between the measurements with a  $r^2$  value of 0.96 is seen. The systematic error and precision of the measurements are examined in the same way as for NO<sub>2</sub>. If a linear relation without a constant term is fitted to the data, the slope of  $0.965 \pm 0.002$  was obtained, indicating Moshiri O<sub>3</sub> data is systematically larger than Rikubetsu O<sub>3</sub> data by 3.5 %. If a linear relation with a constant term is fitted, a slope of 0.973 and an intercept of  $-0.09 \times 10^{19} \text{ cm}^{-2}$  were obtained. A part of the difference can be real, when a sharp gradient of total O<sub>3</sub> amount near Japan is considered. The difference in latitude between the two stations is  $0.9^\circ$  and the zonal mean total O<sub>3</sub> reference model [Keating *et al.*, 1990] has an gradient of about 1 % per degree at latitudes around  $45^\circ\text{N}$ .

The root mean square difference between the two visible spectrometer measurements is  $0.76 \times 10^{19} \text{ cm}^{-2}$ . Assuming that the difference results from the same amount of errors in each data set, the precision of the individual measurement becomes  $1/\sqrt{2}$  of the difference, i.e.  $0.54 \times 10^{19} \text{ cm}^{-2}$ . These values correspond to 3 - 4 % of the slant column amounts. This root mean square difference, however includes a part of the systematic difference between the two measurements described above. If the systematic difference is removed, the precision becomes  $0.37 \times 10^{19} \text{ cm}^{-2}$ , which is to 2 - 3 % of the column. The upper limit precision shown here are about the same as the precision of  $0.4 \times 10^{19} \text{ cm}^{-2}$  estimated from the spectral fitting.

To examine the agreement in the day to day variations, a 31-day running mean value was removed and the residual variations were compared in the same way as for NO<sub>2</sub>. As a result, a clear correlation with a  $r^2$  value of 0.81 was obtained. This suggests that the precision of the measurements is better (smaller) than the general amplitude of the day to day variations at these two sites.

## 2.3 Comparison with Dobson O<sub>3</sub> measurements

Correlation plot between the O<sub>3</sub> values obtained at Moshiri and Sapporo is shown in Figure 4. To avoid the effect of the Pinatubo volcanic aerosols, only the data obtained after September 1992 are used. Closed circles and open circles represent the case in which the direct sun measurement data or indirect sun measurement data are used for the Dobson data. The  $r^2$  value for the cases of the direct sun and indirect sun are 0.91 and 0.85, respectively, suggesting a slightly lower precision of the indirect sun measurements. However, no apparent difference in the slope or interception was seen.

The systematic error in the converted vertical column amount of O<sub>3</sub> cannot be evaluated from the comparison with the Dobson measurements, because it obviously depends on the systematic error in the air mass factor used for the conversion. On the other hand, the random error (precision) of the vertical column amount can be estimated from the comparison with the Dobson measurement. For this estimation, only the Dobson direct sun data is used. When an averaged air mass factor of 17.5 is adopted for the two years Moshiri data, the root mean square of the differences in the vertical column is obtained to be 14.8 Dobson Units, which corresponds to 3 - 6 % of the column. Assuming the precision of 2 % for Dobson direct sun measurements, the difference here suggest the precision of 3 -

5 % for the Moshiri measurements. This is slightly worse than the precision of 2 - 3 % for the slant column obtained from the comparison between the two visible spectrometer measurements when the systematic difference is removed. The worse precision for the vertical column amount could be resulted from the use of a single air mass factor for the two years data. This effect is discussed in detail below.

#### **2.4 Air mass factor for O<sub>3</sub> measurements**

When the systematic difference is removed, the agreement between the two visible spectrometer O<sub>3</sub> data is better than the agreement between the visible spectrometer data and Dobson direct sun data. In the following analyses, only the direct sun data was used for the Dobson measurement. An air mass factor for the O<sub>3</sub> slant column amount at Moshiri was derived by dividing it by the Dobson vertical O<sub>3</sub> amount. Monthly averages of these air mass factors are shown in Figure 5. Vertical bar is one standard deviation within each month. After September 1992, a regular seasonal variation in the air mass factor can be seen in Figure 5. A minimum value appeared in July and August and values were generally high during the winter.

To interpret these variations, an air mass factor was calculated by using a simple single scattering radiative transfer model. The simple assumption is appropriate, because the stratospheric air mass factor for visible radiation less than about 450 nm is relatively insensitive to multiple scattering, surface albedo, refraction, and scattering by background aerosols. Monthly averaged vertical profiles of O<sub>3</sub> mixing ratio and air density obtained by ozonesondes launched from Sapporo by Japan Meteorological Agency were used for this calculation. In Figure 5 the "calculated" air mass factors are shown with "observed" air mass factor. The calculated air mass factor has minimum and maximum values during summer and winter and this is consistent with the observed values. Consequently, the seasonal variation of the vertical profile of O<sub>3</sub> mainly cause the seasonal variation of the air mass factor for the twilight zenith-sky measurements; i.e. a higher peak altitude of O<sub>3</sub> profile in summer results in a lower air mass factor.

The standard deviation of the "observed" air mass factor within each month is 3 - 5 %. This is similar or larger than the amplitude of the seasonal variation of the air mass factor. As already anticipated from the discussion on the seasonal variation, the large standard deviation of the air mass factor within a month mainly resulted from the day to day variation of the vertical profile of O<sub>3</sub>. The results given here confirm the importance of the knowledge of the vertical profile of the absorber in converting the slant column amount into the vertical column, as already pointed by earlier studies. The variations in the "calculated" air mass factor suggest that both the seasonal and day to day variations can result in an additional error of about 2 % for the converted vertical O<sub>3</sub> amounts, when single air mass factor is used for whole season data. As described above, the precision of the slant column O<sub>3</sub> measurements was estimated to be 2 - 3 % from the comparison between the two visible spectrometer measurements. A root sum square of the precision for the slant column and the error in the air mass factor becomes the precision for the converted vertical column of 3 - 4 %. This is consistent with the precision of 3 - 5 % for the vertical columns estimated from the comparison with the Dobson direct sun measurement.

### **3. Star occultation observation of the nighttime altitude distributions of nitrogen oxides**

#### **3.1 Instrumentation**

The observation system consists of a star tracker, 20 cm diameter telescope, multichannel narrow band radiometer and data processor ( Figs.6-8 ). In the balloon experiment, the system will be put in an air tight capsule to keep environmental conditions and to recover. In the star tracker, star position is detected by a multi-anode position sensitive PMT (HAMAMATSU R2846-04). The required precision is about 0.01 degree. In the multichannel radiometer, the light corrected by the telescope is divided by a dichroic mirror and is guided to 2 set of radiometers. Each radiometer consists of a beam splitters, a filter wheel/optical chopper, 6 narrow band interference filters, lenses and 2 PMTs

(HAMAMATSU R1463). It is necessary to separate the absorption due to the nitrogen oxides from the ozone absorption, extinction due to Rayleigh scattering by atmospheric molecules and extinction due to Mie scattering by aerosol particles. We observe several sets of wavelength bands to distinguish the absorption due to the objective molecule from the interference extinction with differential absorption technique. We adopt 616-623-640 nm bands for  $N_2O_5$ , 442-445 nm bands for  $NO_2$ , 551-574 nm bands for ozone. We can also estimate the aerosol profile by measuring these bands. The band width is about 2 nm in full width at half maximum. In the case of the star occultation measurement, the scintillation of star image may lead to fluctuate the light intensity and may result in the precision loss. Since the absorption due to  $NO_3$  molecules is very weak (a few percents), the scintillation effect and the instrumental drift is a serious problem. We use two radiometers to compensate the scintillation effect: one for the large absorption channel and the other for the weak absorption (reference) channel. The role of two radiometer alternate by rotating the filter turret wheel. The filter wheel rotates at the rate of 1800 r.p.m. and it works as a optical chopper to compensate the drift of the instrument by using the phase sensitive detection technique.

### 3.2 Result

Until the end of 1993 fiscal year, the optical component of the star tracker and the radiometer, analog controller of the star tracker, and the on-board signal processing circuit for radiometer had been made.

In 1994 fiscal year, the nighttime variation of nitrogen oxides in the stratosphere was calculated by using a 1 dimensional photochemical model to examine the detailed feasibility of this measurement by using the developing instrument. In this simulation, it was shown that the instrument has a performance enough to detect the nighttime variation of the stratospheric nitrogen oxides. In addition, by using new AFGL absorption line database, it was quantitatively checked that the interference by the absorption of water vapor is not serious problem in the 616-623-640 nm bands. The interface electronics between the on-board signal processing circuit and the balloon PCM telemetry system was made. In addition, the ground support equipment to record the radiometer and star tracker signals by using a personal computer and its software were also developed. Supposing the nighttime stratospheric environment, the ultrasonic motor which is the most significant component of the star tracker was put to the environmental test. No problem was found in the vacuum test. However, since the performance of the motor was unstable in the low-temperature test, we found that the modification of the star tracker was necessary.

In 1995 fiscal year, the star tracker was improved by adopting digital controlled ultra sonic motors which work stably in the low-temperature environment because of its feedback system. In order to keep pressure and temperature conditions during the balloon experiment and in order to recover after it, an air tight capsule was constructed. The capsule is a aluminum cylinder of 80 cm diameter and of 145 cm height, and it has optical window of 30 cm diameter on its side wall. Since the pressure in the capsule is kept to be 1 atm, the strain of the window due to the pressure difference may cause distortion of the star image in the balloon experiment. In some laboratory experiments, we found that the distortion is reduced negligibly by adopting acrylic plastic window of 2.5 cm thickness. We have developed a whole system for a balloon experiment to measure the nighttime variation of nitrogen oxides distribution, and an experiment to check its performance succeeded in a polluted area (Tokyo; we have much nitrogen oxides in the troposphere). However, we have not made any ground-based experiments in the high mountain or a balloon experiment so far. We are planning to make a ground-based experiment in 1996 and a balloon experiment in 1997.

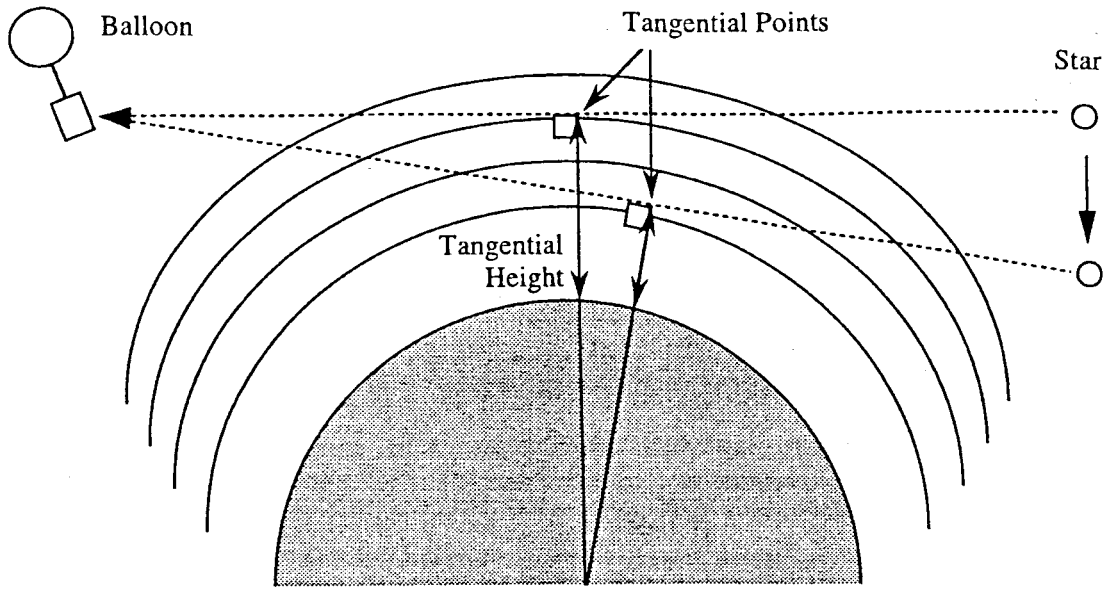


FIG.6 Principle of the star occultation measurements

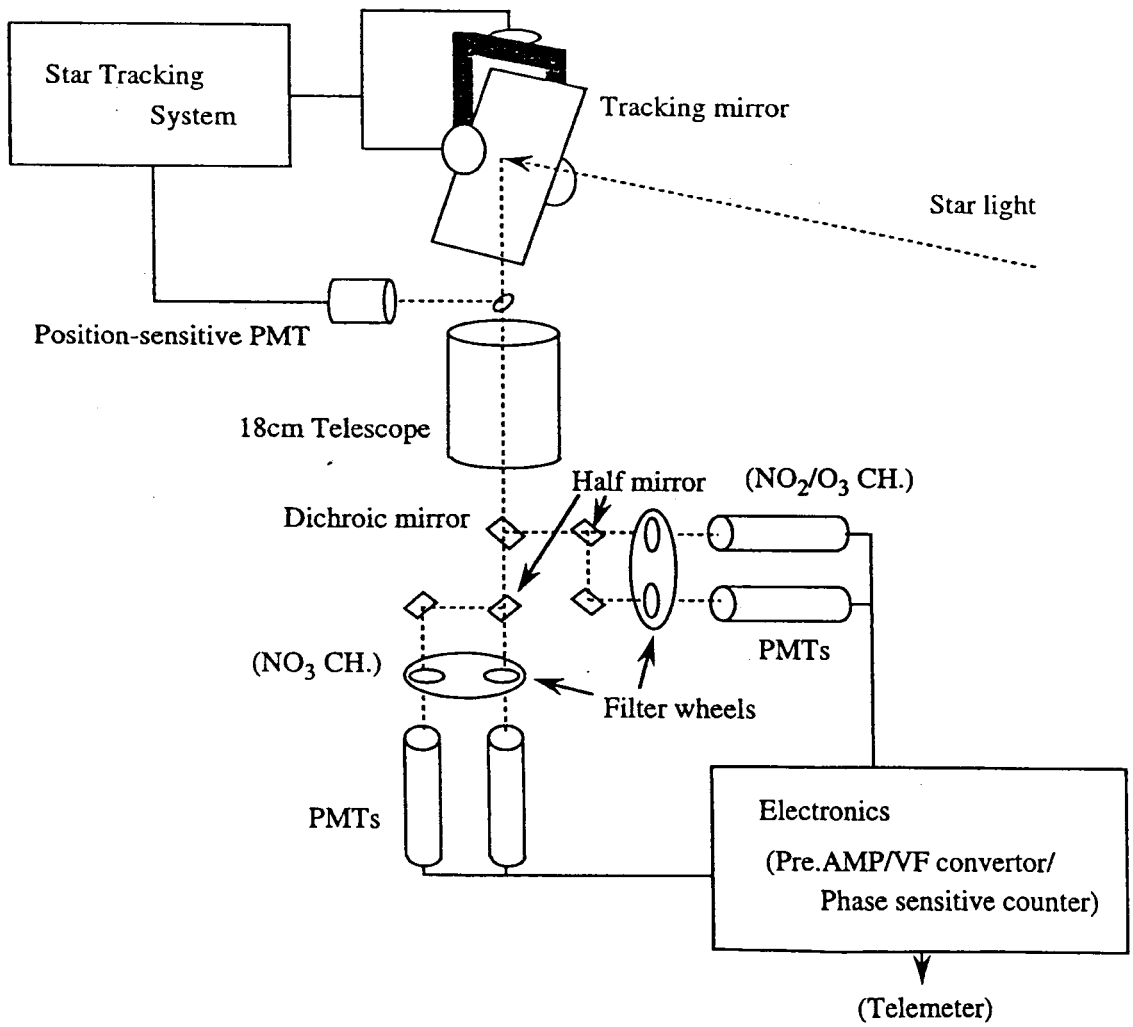


FIG.7 Schematic diagram of the star occultation measurements

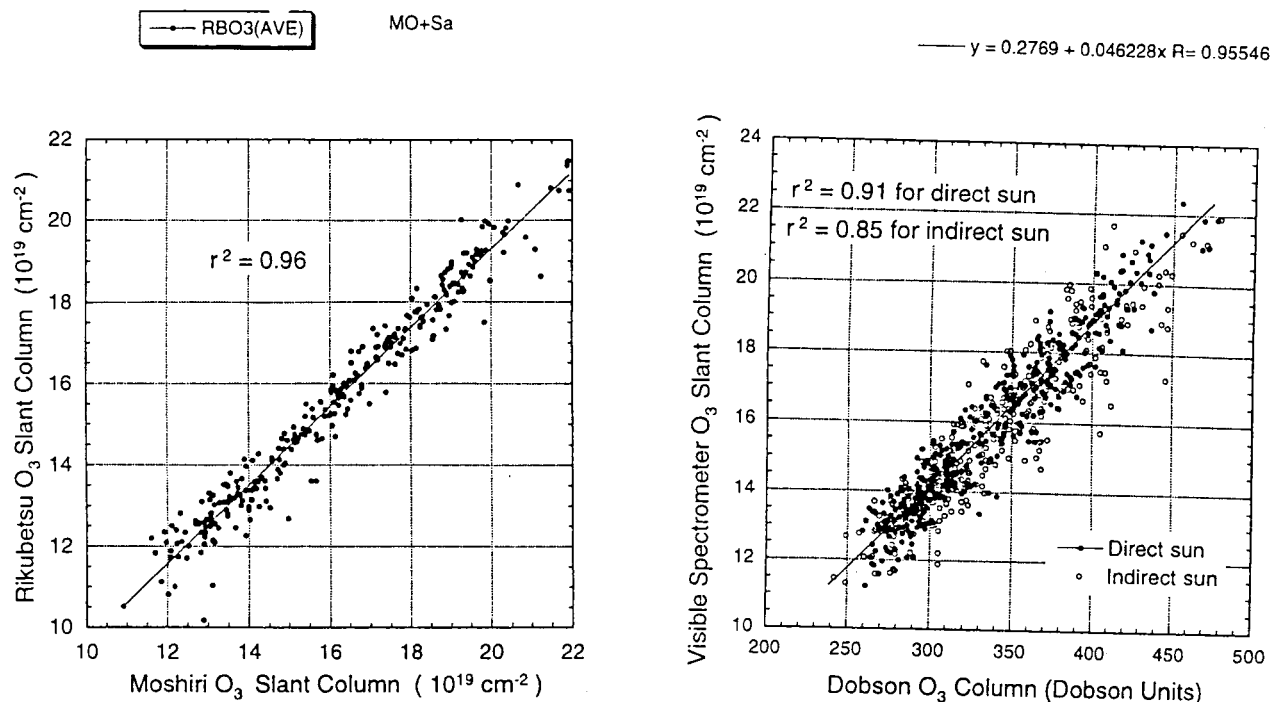


FIG.3 Correlation plot of O<sub>3</sub> slant column amounts for Moshiri and Rikubetsu measurements. A linear relation without a constant term was fitted by a least square calculation resulting in a slope of  $0.965 \pm 0.002$ .

FIG.4 Correlation plot of O<sub>3</sub> slant column amounts obtained by the visible spectrometer at Moshiri and the O<sub>3</sub> vertical column amounts obtained by the Dobson spectrometer at Sapporo. Closed and open circles denote the direct and indirect sun Dobson measurements, respectively.

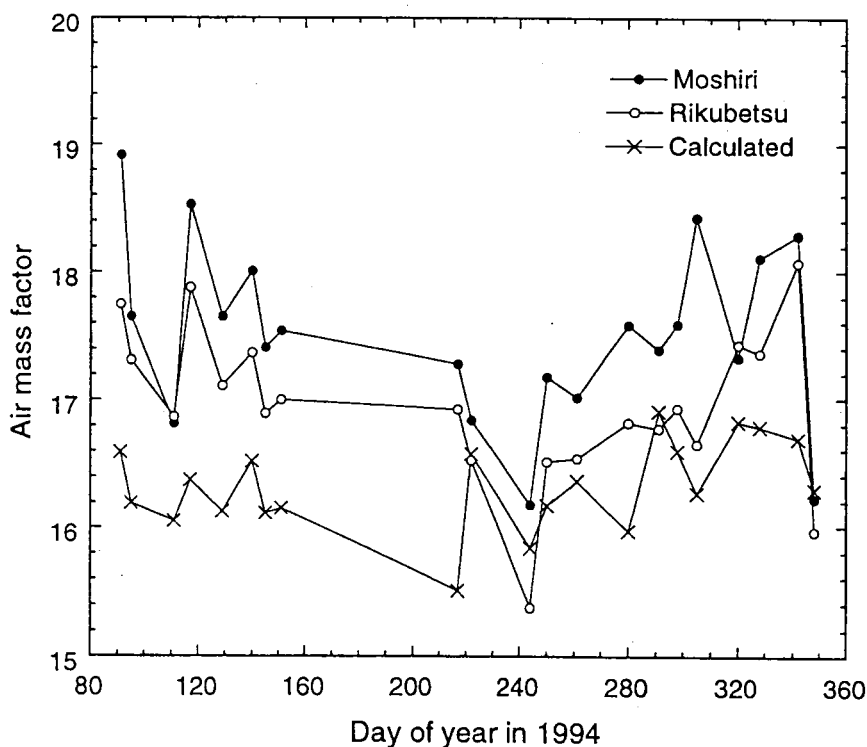


FIG.5 Air mass factor for the O<sub>3</sub> measurements by twilight zenith-sky technique for SZA of 90 degrees. "Observed" air mass factor was obtained by dividing the Moshiri slant column value by the Sapporo Dobson direct sun value. "Calculated" air mass factor was obtained by the vertical profile of O<sub>3</sub> obtained by balloon ozonesondes and simple radiative transfer calculation. Vertical bars for the "Observed" values are one standard deviations within a month.

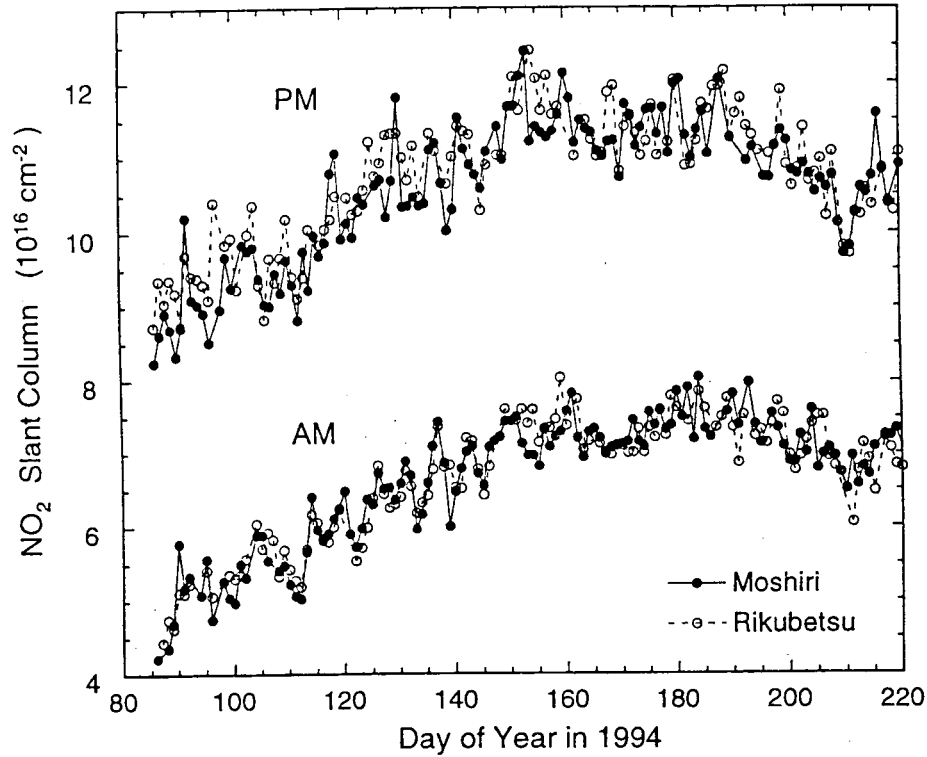


FIG.1 Correlation plot of  $\text{NO}_2$  slant column amounts for Moshiri and Rikubetsu measurements: (a) AM (sunrise) and (b) PM (sunset). A linear relation without a constant term was fitted by a least square calculation resulting in a slope of  $0.999 \pm 0.004$  and  $1.012 \pm 0.004$  for AM and PM data sets, respectively.

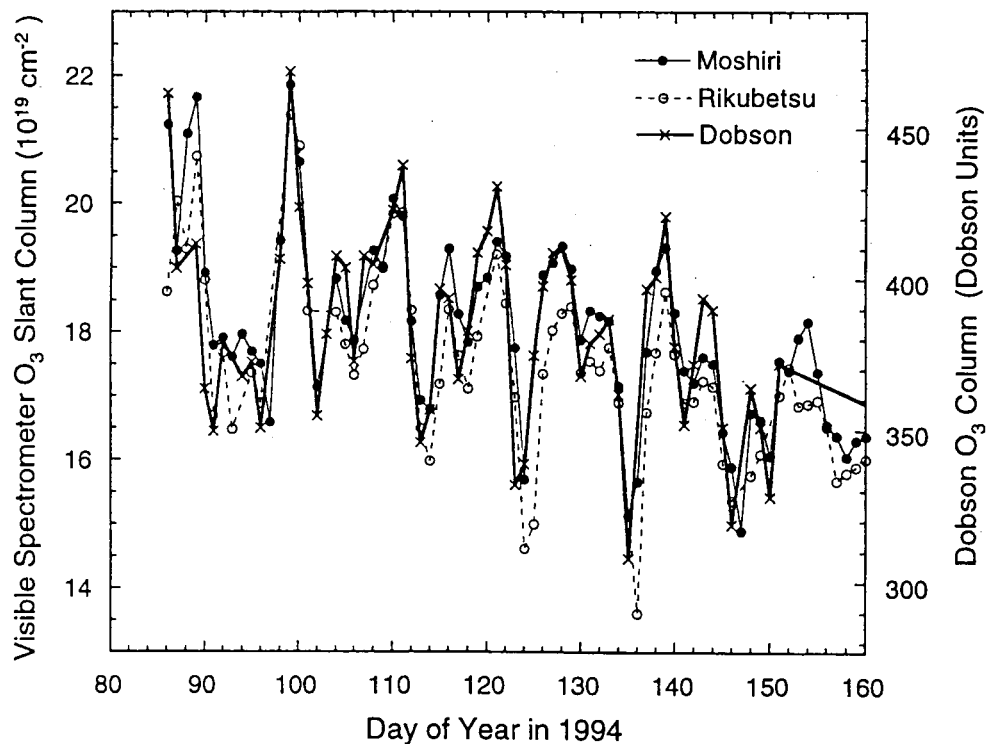


FIG.2 Comparison of the daily  $\text{O}_3$  slant column amounts obtained by the visible spectrometer at Moshiri and the  $\text{O}_3$  vertical column amounts obtained by the Dobson spectrometer at Sapporo. An air mass factor of 17.5 is used to match the Y-axis.



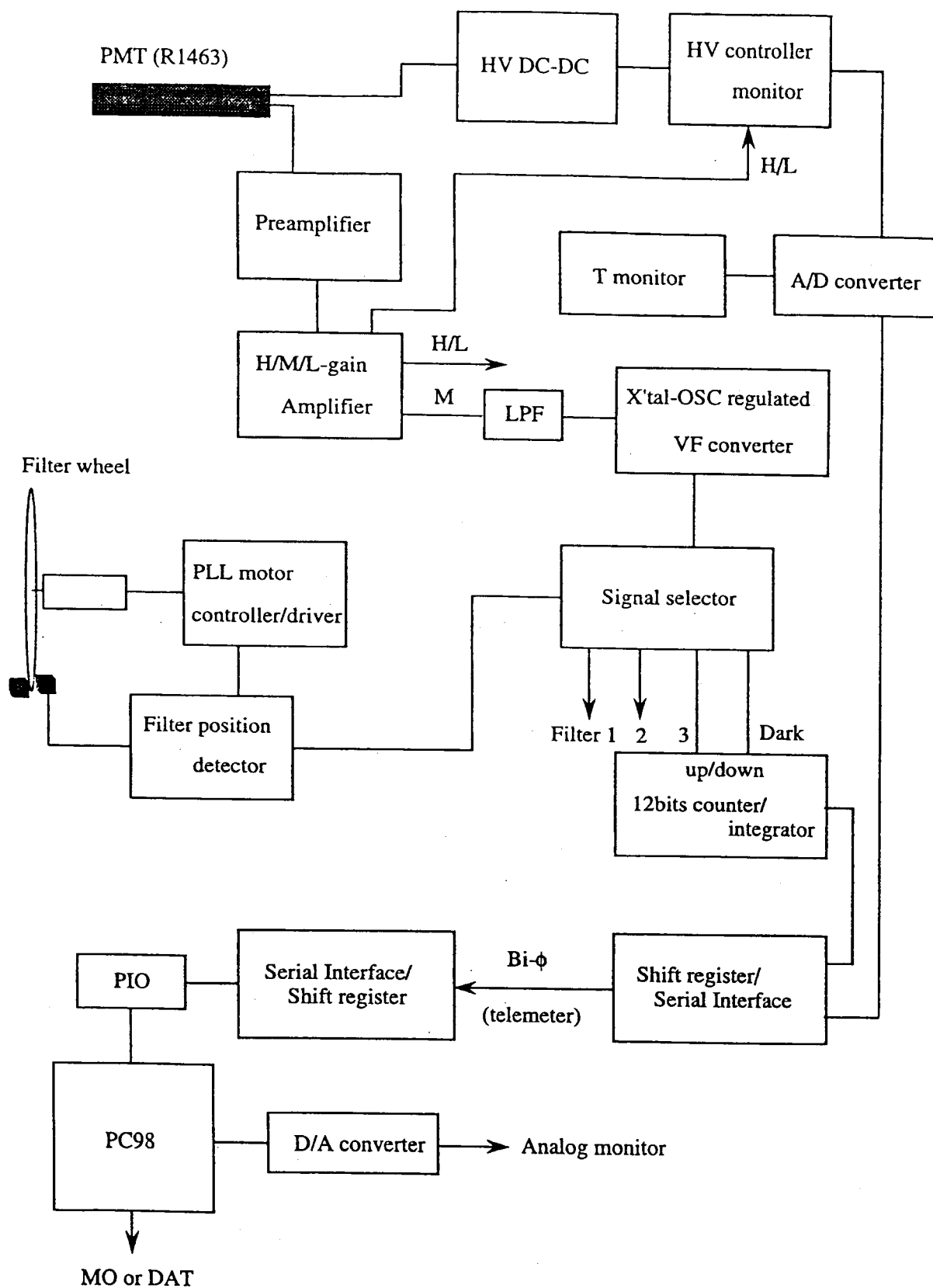


FIG.8 Block diagram of the data processing system